Improving Spectral Reflectance Reconstruction Accuracy using Bootstrap

Alejandro Ribés, Francis Schmitt

Ecole Nationale Supérieure des Télécommunications, Paris, France

Abstract

The idea presented in this paper relates with the generalisation abilities of existing learning-based or indirect spectral reflectance reconstruction methods, which use a priori information about the objects to be imaged. Researchers using this type of methods have characterised and compared their errors over different test sets. However, they do not treat the problem of how to increase the results over these test sets. Using the concept of generalisation we propose an algorithm based on intense random resampling that increases the generalisation capabilities of such methods. This new bootstrap algorithm is applied on a specific operator chosen as a reference, but the algorithm remains general and can be applied to any learning-based reconstruction method. We present simulations and experimental results concerning the performance of the new algorithm.

Introduction

Spectral reflectance reconstruction has to deal with the problems of extrapolation, prediction and estimation of spectral curves. A reconstruction method can obtain bad results when confronted to a particular set of imaged objects while obtaining very good results for others. This is a delicate aspect that has not been treated at the moment on the multispectral scientific community. In fact, we have not seen any reference on the multispectral literature about how the existing methods generalise.

Direct inversion (inversion of the characterised camera model) as presented in [1] and *interpolation* methods as used by [2] or [3] are not considered in the context of this paper because they do not introduce a priori information on the imaged objects. The case of the regularised direct inversion in 4 is different as spectral reflectance curves of the objects to be imaged are introduced to modify the inversion operator. This guarantees a better response over the set of spectral reflectances used as "a priori information", but it still remains the question of what will happen when using other data sets.

The same question arises when building operators on a set of camera responses and their corresponding spectral reflectances, 5, 6 and 7. We deal with these kinds of methods in this article. We call them *learning-based* or *indirect* reconstruction methods. We present an algorithm that increases the generalisation capabilities of the reconstruction operators.

Learning Paradigm

Indirect or learning-based spectral reflectance reconstruction is possible when spectral reflectance curves of a set of P color patches are known and an image of these patches is acquired by a multispectral camera. From this data a set of corresponding pairs (c_p, r_p), for p=1,...,P, is obtained; where c_p is a vector of dimension K containing the camera responses and r_p is a vector of dimension N representing the spectral reflectance of the p-th patch. Corresponding pairs (c_p, r_p) are easy to obtain, for instance professional calibrated color charts as GretagMacbeth[TM] DC are sold with the measurements of the reflectances of their patches. In addition, if a spectroradiometer is available, performing the measure is a fairly simple experiment. Obtaining the camera responses from the known spectral curves of the color chart is just a matter of taking a multispectral image.

Let's now insert in the columns of a NxP matrix $\mathbf{R}$ all the r_i's and in the columns of a KxP matrix $\mathbf{C}$ all their corresponding c_i's. The construction of $\mathbf{R}$ and $\mathbf{C}$ allow

us to write the following solution to the problem of reflectance reconstruction:

$$\Theta^-_{Indirect} = \mathbf{R} \, pinv(\mathbf{C}) , \quad (1)$$

where $pinv(\mathbf{C}) = \mathbf{C}^t \, (\mathbf{C} \, \mathbf{C}^t)^{-1}$, is the pseudo-inverse of the matrix containing the camera responses on its columns.

The method introduced by Burns [5] corresponds to equation (1) where instead of looking for the operator $\Theta^-_{Indirect}$ that matches matrices $\mathbf{C}$ and $\mathbf{R}$, the author looks for an operator that matches another matrix $\mathbf{A}$. This new matrix $\mathbf{A}$ is calculated from $\mathbf{R}$ by Principal Component Analysis (PCA). Also the *non-averaged pseudo-inverse* method in [6] corresponds to equation (1) where the matrices $\mathbf{R}$ and $\mathbf{C}$ are large matrices and $\mathbf{C}$ contains original noisy camera responses without any low-pass filtering. Consequently, in order to present our proposed algorithm we choose the operator $\Theta^-_{Indirect}$ as reference for the learning-based paradigm.

Proposed algorithm

The proposed algorithm uses the concept of bootstrap presented in [8]. The algorithm resamples simultaneously matrices $\mathbf{R}$ and $\mathbf{C}$ by using a random selection of their columns. The probability distribution used for the selection is uniform. We then call *resample*(.) a function taking a matrix and returning another matrix with randomly resampled columns. The function *resample*(.) transforms equally $\mathbf{R}$ and $\mathbf{C}$ by using the same random selection in each iteration. This condition is respected as, by definition, the two matrices contain corresponding columns. We note that the obtained matrices will contain repeated columns. Consequently, some columns of the original matrices will not be present on their resampled version.

The proposed algorithm consists in building a reconstruction operator using the resampled matrices obtained from $\mathbf{R}$ and $\mathbf{C}$. A large number of operators can be calculated along with their errors over a test set of data, $\mathbf{R}_{test}$ and $\mathbf{C}_{test}$. Test data are necessarily to be

different from $\mathbf{R}$ and $\mathbf{C}$. Afterwards the operator showing the lowest Root Mean Square (RMS) error on the test set is chosen.

The algorithm in pseudo-code is as follows:

> **For** i=1,…,*Iter*
> $\quad \mathbf{R}_i = resample(\mathbf{R})$
> $\quad \mathbf{C}_i = resample(\mathbf{C})$
> $\quad \Theta_i = \mathbf{R}_i \, pinv(\mathbf{C}_i)$
> $\quad error_i = \| \Theta_i \, \mathbf{C}_{test} - \mathbf{R}_{test} \|^2$
> **End For**
> Choose Θ_i having the smallest $error_i$

where *Iter* is the number of iterations.

Spectral Reflectance Databases

In this article we use several databases of spectral reflectances. We present them in the following. The first three of them are kindly provided by D. Saunders from The National Gallery, London, the last one is downloaded from the Color Research Laboratory at University of Joensuu 9:

- The "Kremer" database contains 184 spectral curves of pigments produced by Kremer Pigmente, Germany.

- The "Selected Artists" database contains 67 pigments chosen among a collection of artist's paintings.

- The "Restoration" database contains a selection of 64 pigments used in oil painting restoration.

- The "Munsell" database is not issue from the same canvas painting environment. It contains spectral curves corresponding to 1269 matte Munsell colour chart samples.

- The "MacbethDC" database. We have scanned in our laboratory a *GretagMacbethTM DC color chart* using a Minolta CS-100 spectroradiometer. From this experiment we obtained 200 spectral curves.

- The "Pine Tree" database. This database contains 370 forest spectral reflectances, see 9. We include this database in some our tests because its nature is fundamentally different from the others we presented above.

Simulations

We applied the presented bootstrap algorithm introduced using *Iter*=100 to some spectral reflectance databases. In this section, to illustrate the improvements obtained in our experiments we choose **R** as the matrix containing the spectral reflectances of the MacbethDC dataset. The corresponding matrix **C** is calculated by simulation considering a multispectral system with seven equidistributed Gaussian-shaped filters on the visible part of the spectrum. Twelve bits quantization is introduced on the system. The test reflectances used, $\mathbf{R}_{test}$, are the Kremer dataset. $\mathbf{C}_{test}$ is calculated by simulation exactly as for **C**.

Table 1. Comparing spectral accuracy results before and after bootstrapping

	MacbethDC	Kremer
No bootstrap	0.0001884	0.001081
After bootstrap	0.0002069	0.000744

Table 1 presents the results of the application of the algorithm on the training set of the reconstruction method and on the test set of our algorithm. We found that it indeed reduces the RMS error on the test set but the error is augmented on the set used to build the operator. This increase of the reconstruction error on **R** is not necessarily bad. In fact, poor generalisation implies normally high specialisation on a set of data used for training. In fact, by just considering data presented on Table 1 we cannot know if the generalisation capabilities of the built operator are increased. We then present on Table 2 the results obtained using the bootstrap operator optimised on the Kremer database and applied to: Selected Artists, Restoration, Munsell, and Pine Tree datasets. The effect on these datasets is very positive, a reduction of the RMS spectral error is clear on all cases. The mean increase in accuracy is 29.6% that can be considered very significant, even more when considering that they are generalisation results and the used datasets come from very different origins.

Table 2. Generalisation results before and after bootstrapping

	Selected Artists	Restoration
No bootstrap	0.0006915	0.0006445
After bootstrap	0.0004822	0.0003969
Improvement	30.3%	38.4%
	Munsell	**Pine Tree**
No bootstrap	0.0001538	0.0010293
After bootstrap	0.0001326	0.0006592
Improvement	13.8%	36.0%

Even if the reduction of the RMS errors presented on Table 2 is very positive for *Iter*=100 iterations we wanted to know if it was possible to improve the results further. For this we applied our algorithm iteratively, the best $\mathbf{R}_i$ matrix found after *Iter*=100 iterations of the algorithm being used as the matrix **R** for the next set of *Iter*=100 iterations. This strategy appears indeed to further reduce the error. Then, we decided to study closer the effect of the iteration of the algorithm. On the top panel of Figure 1 we can see the evolution of the error on the test dataset $\mathbf{R}_{test}$ while iterating. Twenty algorithm iterations are enough to see that the error is reduced till a plateau is reached after 5 iterations. On the bottom panel of Figure 1 the evolution of the reconstruction error on **R** (the set used to train the reconstruction method) is shown. This error increases on each iteration and also reaches a plateau after 15 iterations. It is important to note that the plateau of error reduction on $\mathbf{R}_{test}$ is reached before the plateau of error increase on **R**.

On Figure 2 we present in a similar graph as on top panel of Figure 1 the RMS spectral error on the Selected Artists, Restoration, Munsell, and Pine Tree Leaves datasets. We can see that the iteration of our algorithm also reduces the error on these datasets. A plateau or a minimum is reached around 5 iterations as for $\mathbf{R}_{test}$, the Kremer test set. An exception appears for the Pine Tree dataset that continues decreasing its error. The behaviour of the algorithm observed on these experiments indicates that the optimum number of iterations is five for this case. Iterating more does not decreases the generalisation capabilities of the

reconstruction operation. On the contrary too many iterations degrade the reconstruction quality on the training set of the method and also on some datasets used to test the generalisation.

Before concluding this section we quantify the improvements introduce for the proposed bootstrap based method. If we call *rms* the RMS reconstruction error without bootstrap and rms_b the RMS error obtained once the bootstrap has been applied, we can then easily calculate the per cent of improvement as:

$$\%_{improvement} = \frac{rms - rms_b}{rms} \times 100 \qquad (2)$$

On Table 3 we present the results obtained after five iterations of the proposed algorithm (with *Iter*=100). We present for comparison the results when the algorithm is not used and the calculated per cent of improvement using equation (2). The results for generalisation appear to be very satisfactory. We also observe that after 5 bootstrap iterations the RMS error is much more equally distributed on the various datasets used for testing generalisation.

Table 3. RMS errors before and after bootstrapping (5 iterations) and % of improvement.

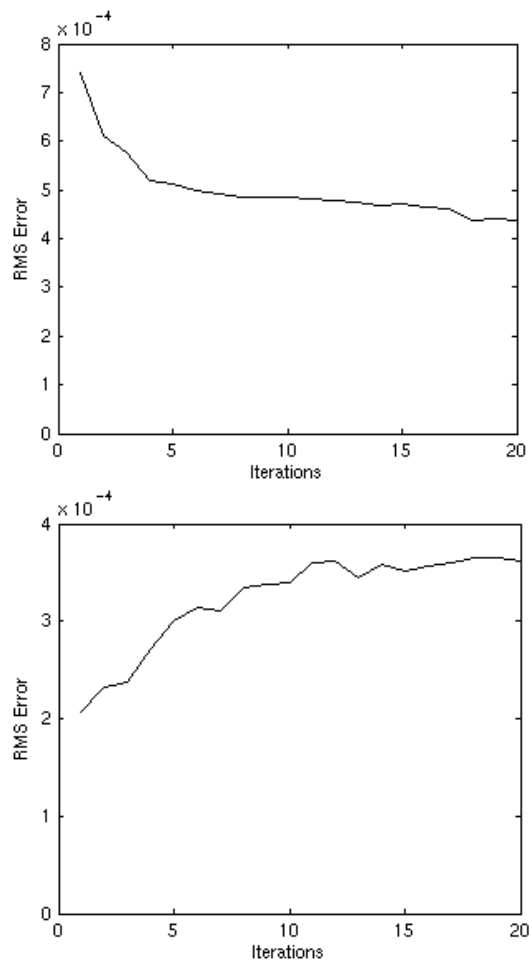|	MacbethDC	Kremer
No bootstrap	0.0001884	0.0010810
5 bootstraps	0.0003009	0.0005168
Improvement	-59.7%	52.2%
	Selected Artists	Restoration
No bootstrap	0.0006915	0.0006445
5 bootstraps	0.0003467	0.0002742
Improvement	49.9%	57.5%
	Munsell	Pine Tree
No bootstrap	0.0001538	0.0010293
5 bootstraps	0.0001141	0.0003194
Improvement	25.8%	69.0%

Figure 1. RMS error evolution when iterating the bootstrap based algorithm several times. (top panel) Kremer data set used as test for the bootstrap, (bottom panel) MacbethDC data set used as learning set for the reconstruction operator.
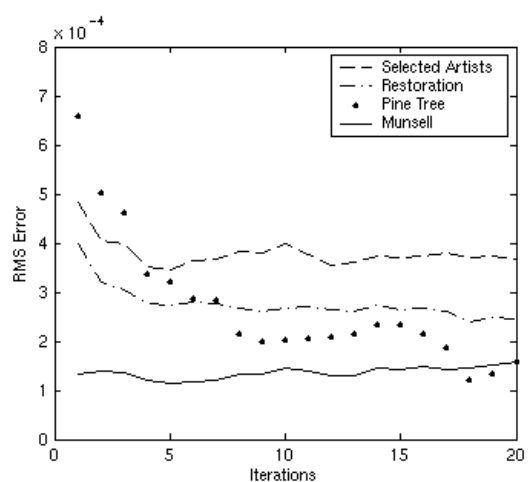

Figure 2. RMS error evolution on other data sets.

Experimental Results

An experiment was performed using the multispectral camera developed at the European project CRISATEL, see [10] for reference. An image of the CRISATEL chart (also developed in the context of the project) was taken by the CRISATEL acquisition system.

The CRISATEL chart is a juxtaposition of three sets of colour patches, each set contains the same patches sorted in the same way. The difference between these sets is the application of varnish over the pigments. The first set has no varnish, the second set has a thin layer of matt varnish and the third set has a layer of brilliant varnish. Each set contains 117 colour patches, 81 are colour patches and 36 form a greyscale. The CRISATEL chart was measured by different spectrophotometers at London and Paris, see *chapter 2* of 11 for more details. We take the 117 non varnish patches of the CRISATEL chart and analyse them to obtain two different kinds of data:

1. A matrix containing 117 columns with the mean camera responses of each colour patch.
2. A matrix containing 117xS columns containing non averaged camera responses, S being the quantity of pixels analysed into each colour patch.

In order to use the learning-based reconstruction paradigm we divide the CRISATEL chart into two sets: one will be used for training and the other for testing. This leads to four different sets: averaged train set, non-averaged train set, averaged test set and non-averaged test set. The train and test sets have the same size. The original matrix has been divided into two non intersecting sets by taking even elements for one set and odd for the other. We note that the averaged camera responses sets can be considered as less influenced by noise than the non-averaged ones that present a more realistic situation.

In Table 4 we present spectral reconstruction errors (using the L_1 metric) obtained by using different learning-based spectral reflectance reconstruction techniques, they are: $\Theta^-_{Indirect}$, the operator presented in equation (1); Θ^-_{PCA}, the application of PCA to matrix **R** on equation (1), see [5]; Θ^-_{noisy},

the non-averaged operator [6]; and $\Theta^-_{bootstrap}$, the proposed bootstrapped operator.

Table 4. Results of four learning-based spectral reconstruction operators over the CRISATEL colour chart.

	Train set	Mean test set	Non averaged test set
$\Theta^-_{Indirect}$	0.010225	0.014875	0.015390
Θ^-_{PCA}	0.010770	0.015380	0.015878
Θ^-_{noisy}	0.010225	0.014741	0.015258
$\Theta^-_{bootstrap}$	0.010878	0.014594	0.015176

The results presented in Table 4 indicate that most methods perform similarly. The bootstrap method performs slightly better than the others but the increment is very small. This is due to the training and test set used all belong to the same kind of spectral reflectance: art pigments. However the results presented in Table 4 only concern mean values. In Figure 3 we present the error histograms of the four compared methods. The error histogram of the bootstrapped operator, shown in panel (c), appears to be slightly better distributed than the other methods. This is seen as the histogram bars in (c) are grouped towards the left side of the histogram following a Gaussian like distribution.
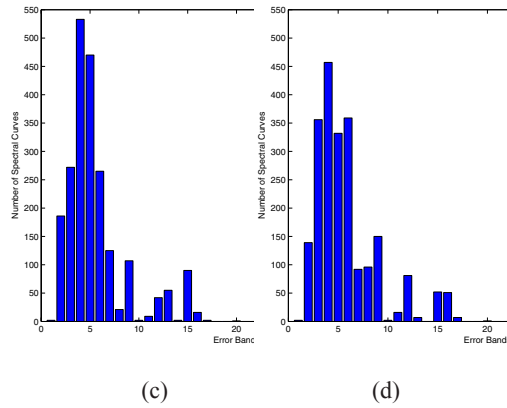

(a) (b)

(c)　　　　　　　(d)
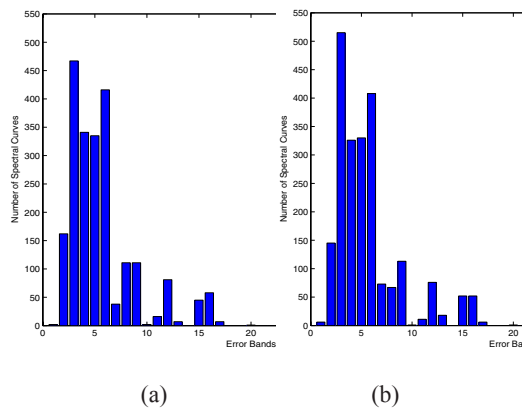
Figure 3. Error histograms of different spectral reconstruction methods: (a) $\Theta^-_{Indirect}$, (b) Θ^-_{noisy} , (c) $\Theta^-_{bootstrap}$, (d) Θ^-_{PCA} .

This experiment is just a preliminary test. Even if already positive, our experiment is to be extended using other charts of different materials.

Conclusion

We have proposed a method for improving the generalisation capabilities of linear reconstruction operators by using bootstrap. To our knowledge, it is the first time that such an approach is taken on spectral reflectance reconstruction. We have tested the method by simulation and using the CRISATEL acquisition system. The obtained results are satisfactory. Even if the tests have been performed using a specific operator, the algorithm remains general and is applicable to any learning-based reconstruction method using a priori information over the imaged objects.

Acknowledgements

References

1. Pratt W. K., Mancill C. E. [1976] *Spectral estimation techniques for the spectral calibration of a color image scanner* Appl. Opt., 15, 1, (1976) 73-75

2. Herzog G. P., Hill B. [2003] *Multispectral Imaging and its Applications in the Textile Industry and Related Fields*. In proceedings of PICS03: The Digital Photography Conference. pp. 258-263. Rochester, USA.

3. Keusen T. [1996] *Multispectral color system with an encoding format compatible with the conventional tristimulus model*. Journal of Imaging Science and Technology, 40(0), pp. 510-515.

4. Hardeberg J.Y., Schmitt F., Brettel H., Crettez J., Maître H. [1999] *Multispectral image acquisition and simulation of illuminant changes*. Chapter in MacDonald L. W. and Luo M. R. *(edited by)*, *Color Imaging. Vision and Technology* John Wiley & Sons, Ltd, pp. 145-164.

5. Burns P. D. [1997] *Analysis of image noise in multitraitement color acquisition*. Ph.D. thesis, Center for Imaging Science, Rochester Institute of Technology, USA.

6. Imai F. H., Taplin L. A. and E. A. Day. [2002] *Comparison of the accuracy of various transformations from multi-band image to spectral reflectance*. Technical Report of the Rochester Institute of Technology. Rochester, USA.

7. Ribés A., and Schmitt F. [2003] A Fully Automatic method for the Reconstruction of Spectral Reflectance Curves by using Mixture Density Networks, *Pattern Recognition Letters*, **24** (11), pp. 1691-1701.

8. Efron, B. [1979] Bootstrap Methods: Another Look at the Jacknife. *Annals of Statistics*, 7, pp. 1-26.

9. Jaaskelainen, T., Silvennoinen, R., Hiltunen, J. and Parkkinen, J. P. S. [1994] Classification of the reflectance spectra of pine, spruce, and birch. *Applied Optics*, Vol. 33, No. 12, 20, pp. 2356-2362.

10. Ribés A., Schmitt F., Pillay R., Lahanier C. [2005] *Calibration, Spectral Reconstruction and Illuminant Simulation for CRISATEL: an Art Paint Multispectral Acquisition System*. Journal of Imaging Science and Technology, **49** (6) (2005) p. 463-473.

11. Ribés A. [2003] *Multispectral Analysis and Spectral Reflectance Reconstruction of Art Paintings*. Ph.D. thesis, Ecole Nationale Supérieure des Télécommunications, Paris, France.